Image Cover Sheet

CLASSIFICATION	SYSTEM NUMBER
UNCLASSIFIED	510036

TITLE

A METHOD FOR TRACKING AND REMOVING MOTION ARTIFACTS IN COMPUTED TOMOGRAPHY IMAGING SYSTEMS

System Number:

Patron Number:

Requester:

Notes:

DSIS Use only:

Deliver to:

DCIEM No. 98-CR-52

A METHOD FOR TRACKING AND REMOVING MOTION ARTIFACTS IN COMPUTED TOMOGRAPHY IMAGING SYSTEMS

by

A. C. Dhanantwari * **and S. Stergiopoulos** †

* Department of Electrical and Computer Engineering, The University of Western Ontario, London, Ontario, N6A 5B9, CANADA; acdhanan@julian.uwo.ca;

† Defence and Civil Institute of Environmental Medicine, 1133 Sheppard Ave. W., P.O Box 2000, Toronto, Ontario, M3M 3B9, CANADA; stergios@dciem.dnd.ca;

Amar C. Dhanantwari *
57 Stillwater Cr.
North York, Ontario
M2R 3S3

Purchase Order #~~247-071~~ (247071)

on behalf of
DEPARTMENT OF NATIONAL DEFENCE

as represented by
Defence and Civil Institute of Environmental Medicine †
1133 Sheppard Avenue West
Toronto, Ontario, Canada
M3M 3B9

DCIEM Scientific Authority:
S. Stergiopoulos
(416) 635 2049

October 1998

DCIEM No. 98-CR-52

A METHOD FOR TRACKING AND REMOVING MOTION ARTIFACTS IN COMPUTED TOMOGRAPHY IMAGING SYSTEMS

by

A. C. Dhanantwari * **and S. Stergiopoulos** †

* Department of Electrical and Computer Engineering, The University of Western Ontario, London, Ontario, N6A 5B9, CANADA; acdhanan@julian.uwo.ca;

† Defence and Civil Institute of Environmental Medicine, 1133 Sheppard Ave. W., P.O Box 2000, Toronto, Ontario, M3M 3B9, CANADA; stergios@dciem.dnd.ca;

Amar C. Dhanantwari *
57 Stillwater Cr.
North York, Ontario
M2R 3S3

Purchase Order #~~247-071~~ (247071)

on behalf of
DEPARTMENT OF NATIONAL DEFENCE

as represented by
Defence and Civil Institute of Environmental Medicine †
1133 Sheppard Avenue West
Toronto, Ontario, Canada
M3M 3B9

DCIEM Scientific Authority:
S. Stergiopoulos
(416) 635 2049

October 1998

EXECUTIVE SUMMARY

Computed Tomography in medical applications is an imaging modality that reproduces transverse cross sections or "slices" of the human body. The patient is placed in between an x-ray source and an array of sensors, this last measuring the amount of radiation that passes through the body. During the data acquisition, source and detectors move around the patient, 360 degrees, resulting in a large number of X-ray projections. Finally, from this set of data and by applying image reconstruction techniques an image of the body's cross-section of interest is reconstructed. This process requires stationarity, which is always being violated by organ motion during the relatively long data acquisition process, which usually takes about one second. This affects seriously the quality of the final reconstructed image, which presents blurring effects, the so-called motion artifacts, that may prevent reliable diagnosis. The intuitive solution to this approach is to speed up the data acquisition process, so that the motion effects would become negligible. This requirement cannot be met even by the most advanced conventional CT scanner today. The only scanner concept that delivers this kind of speed is the Electron Beam CT (EBCT) which provides very poor reconstructed images. Moreover, the system and maintenance costs are very high to allow for commercial viability. As solution several techniques have been proposed that require a priori knowledge of the motion characteristics. This paper proposes an assumption-free method to eliminate the motion artifacts: it uses the Overlap Correlator concept to extract the motion information from the CT raw data and an Adaptive Noise Canceller to remove the organ motion effects at the sensor level before applying the conventional image reconstruction procedure. The work is the result of an European (Esprit) project titled "NEW ROENTGEN". Real and synthetic data tests demonstrate the validity of this approach and also show that it is possible to be implemented in current CT systems.

I INTRODUCTION

In standard computerized tomography, image reconstruction is performed using projection data that are acquired in a time sequential manner. Organ motion (cardiac motion, blood flow, lung motion due to respiration, patient's restlessness etc.) during data acquisition produces artifacts, which appear as a blurring effect in the reconstructed image, and may lead to inaccurate diagnosis [1,2,3]. The intuitive solution to this problem is to speed up the data acquisition process, so that the motion effects become negligible. However, faster CT scanners tend to be significantly more costly and, with current x-ray tube technology, the scan times that are required are simply not realizable. Signal processing algorithms to account for organ motion artifacts are therefore needed. Several mathematical techniques have been proposed as a solution to this problem. These techniques usually assume a simplistic linear model for the motion, such as translational, rotational or linear expansion [1]. Some techniques model the motion as a periodic sequence and take projections at a particular point in the motion cycle to achieve the effect of scanning a stationary object. However, in practical applications motion is much more complex, and these techniques are useful in a very limited number of cases. A more general technique attempts to iteratively suppress the motion effects from the projection data [2]. This method attempts to reduce the assumed spectral characteristics of the motion artifact. It, however, depends on knowing some properties of the motion a-priori, and requires a number of iterations to converge. The spectral properties of some complex form of motion may not necessarily correspond to the model used in this algorithm. Moreover, without proper initialization, the convergence period could be long. The approach presented in this paper uses the spatial overlap correlator [4,5,7,8] scheme to accurately sample the information due to organ motion from the sensor time series. The adaptive interference canceller [6,7] is then used to adaptively remove the motion effects from this sensor data. This combination scheme has been successfully tested with both real and synthetic data sets.

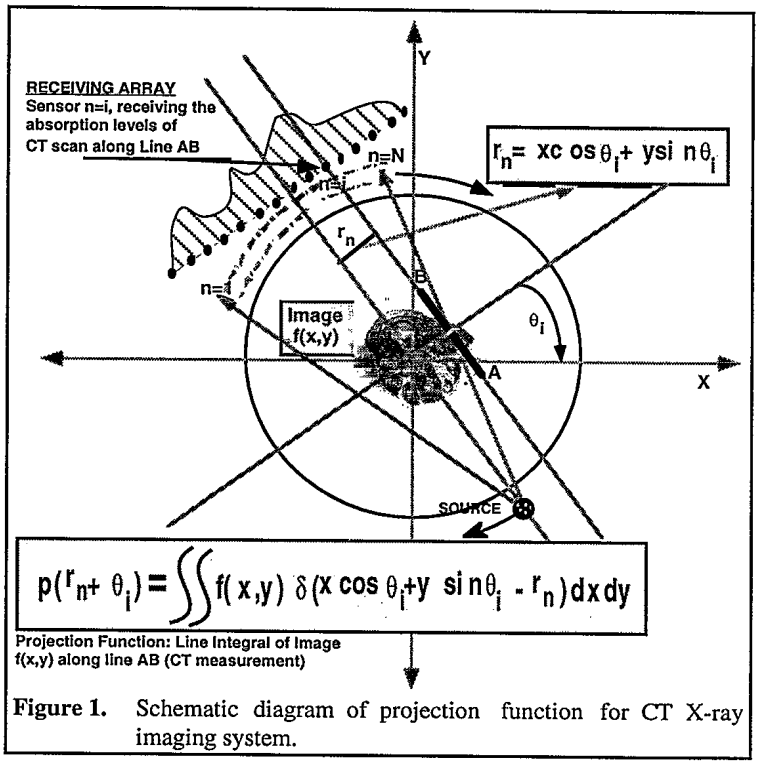

Figure 1. Schematic diagram of projection function for CT X-ray imaging system.

II THEORETICAL REMARKS

Definition of Parameters: The data acquisition process in CT applications is depicted in Figure 1. The projection measurements, $\{ p_n(r_n, \theta_i), (n = 1, \ldots, N)\}$, shown schematically in this figure, are defined as the line integrals along lines passing through the image f(x,y) (e.g. line AB):

$$p_n(r_n, \theta_i) = \iint f(x,y)\,\delta\{x\cos\theta_i + y\sin\theta_i - r_n\}\,dxdy \qquad (1)$$

which is applicable for parallel beam projection CT scanners. The angular step increment between two successive projections of the X-ray scanner is defined by: $\Delta\theta = 2\pi/M$, where M is the number of projections during the period T required for one full rotation of the source and receiving array around the tomography area of the image f(x,y).

For fan beam scanners, the projection function includes the following transformations to account for the geometry of the fan beam, as shown in Figure 2:

$$r_n = R\sin\sigma_n , \qquad \theta_i = \sigma_n + \beta_i .$$

The projection function is now defined by [10]:

$$g_n(\sigma_n, \beta_i) = p_n\{[r_n = R\sin\sigma_n],[\theta_i = \sigma_n + \beta_i]\} . \tag{2}$$

In the image reconstruction process, the pixel I(j,k) of the actual image shown at the right and side of Figure 2, corresponds to the Cartesian point (x_j, y_k) in the CT scan plane. I(j,k) is given by:

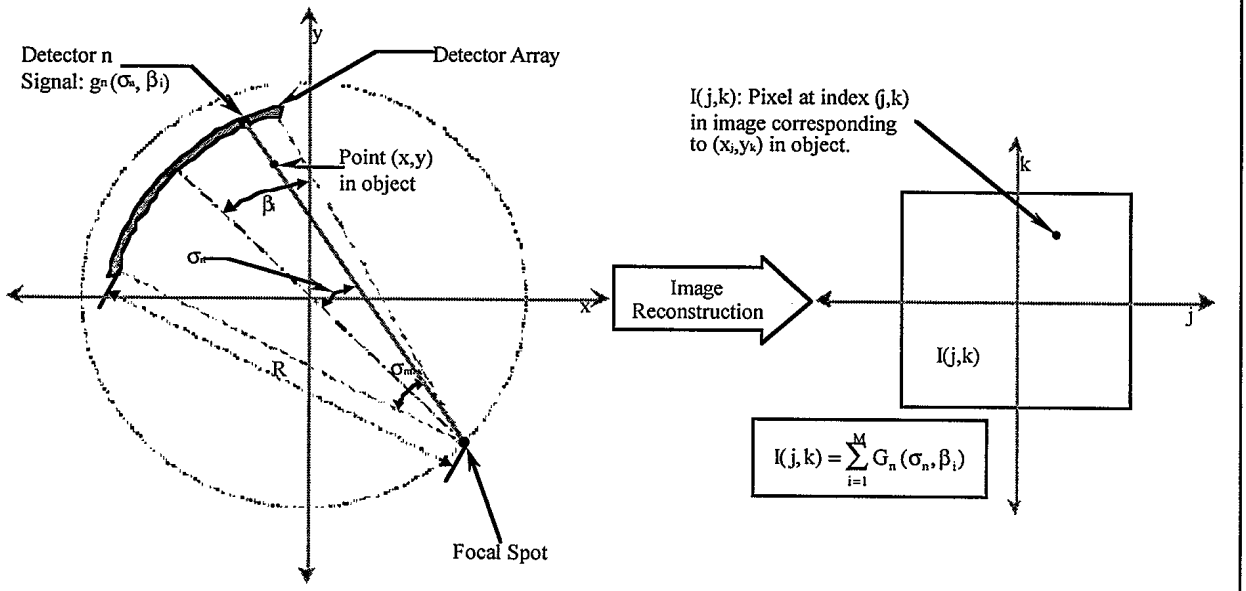

Figure 2. Schematic Diagram of Fan-Beam projections and reconstruction in CT X-ray imaging system.

$$I(j,k) = \sum_{i=1}^{M} G_n(\sigma_n, \beta_i) , \tag{3}$$

where $G_n(\sigma_n, \beta_i)$ is the filtered version of the projection $g_n(\sigma_n, \beta_i)$. The filter function used is the Ram-Lak filter [10], cascaded with the Parzen window [11]. The angle σ_n, which defines the detector that samples the projection through the point (x_j, y_k) for a given projection angle β_i, is defined by:

$$\sigma_n = \mathrm{Tan}^{-1}\left[\frac{r_d \sin(\beta_i - \varphi)}{R + r_d\cos(\beta_i - \varphi)}\right], \quad \frac{-\pi}{2} \le (\beta_i - \varphi) < \frac{\pi}{2} \qquad \text{or,}$$

$$\sigma_n = \mathrm{Tan}^{-1}\left[\frac{r_d \sin(\varphi - \beta_i)}{R + r_d\cos(\varphi - \beta_i)}\right], \quad \frac{\pi}{2} \le (\beta_i - \varphi) < \frac{3\pi}{2}, \tag{4}$$

where (r_d, φ) is the polar representation of (x_j, y_k).

Spatial Overlap Correlator: The problem of motion artifacts is well known in other type of real time imaging systems such as RADAR satellites and SONARs [7]. In SONAR applications [7], it has been shown that the spatial overlap correlator increases the angular resolution (array gain) and reduces artifacts that are caused by scattering and, target's and receiving-array's motion effects. The approach of generating a synthetic aperture is based on computing an appropriate phase correction factor to coherently synthesize spatial measurements [7]. Extending this scheme to the case of a CT application is not straightforward. The computation of the correction is still based on the comparison of spatially overlapping measurements. This phase correction factor compensates for the phase or amplitude fluctuations caused by the subject's organ-motion effects and tracks the information due to organ-motion such as the heart and lungs. Shown in Figure 3, is the concept of the spatial overlap correlator for CT applications. In a sense, this is a data acquisition scheme to obtain an estimate of the motion information for subsequent removal. As shown in Figure 2, the scheme uses two sources, and an array receiver. The system of two sources - array receiver performs the data acquisition process in a conventional manner. Specifically, at time t_0, the array receiver and the two sources are at spatial locations s_0 and s_1 respectively, shown by the dark dots in Figure 3. At time $(t_0 + \Delta t)$ they will be at locations s_1 and s_2, shown by the lighter dots in Figure 3. The process is repeated throughout the data acquisition period T.

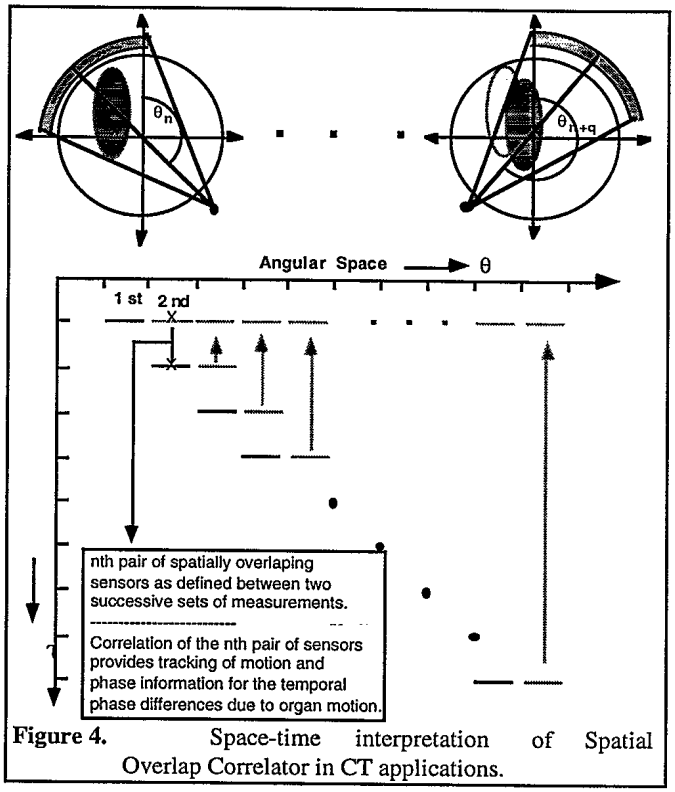

Figure 4. Space-time interpretation of Spatial Overlap Correlator in CT applications.

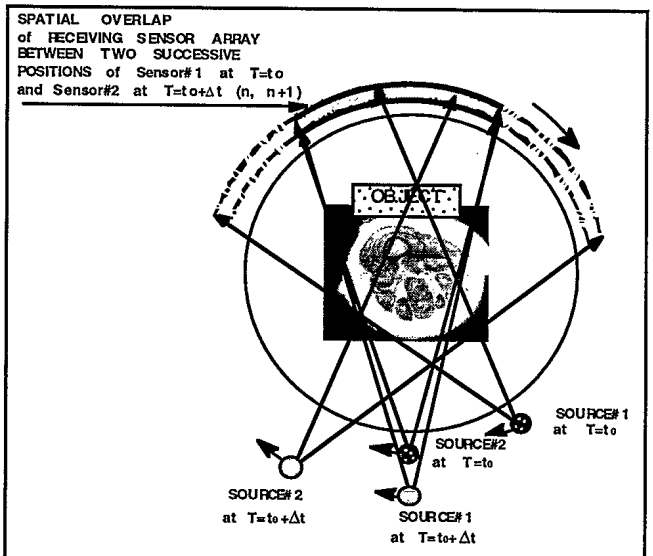

Figure 3. Concept of Spatial Overlap Correlator for CT X-ray scanners.

From this arrangement, for a stationary image, it is evident that this two source configuration will provide spatially identical sets of measurements at all spatial locations, despite being taken at two successive moments in time, separated by Δt. The time interval $\Delta t = T/M$, is the elapsed time between two successive firings of the X-ray. In the example of Figure 3, measurements for spatial location s_1 are obtained at time t_0 and $(t_0 + \Delta t)$. Comparison (or correlation) of the two spatially overlapping measurements will provide measurements associated with any organ motion that may have occurred

during the time Δt. More specifically, suppose

$$\{ p_{n_{s1}}(r(t),\theta(t),t_o),\ (n_{s1} = q,\ q+1,..,N),\} \qquad \text{and}$$
$$\{ p_{n_{s2}}(r(t),\theta(t),t_o + \Delta t),\ (n_{s2} = 1,2,..,N-q),\} \tag{5}$$

are the (N-q) spatially overlapping projection data received by the N-element array at the two successive moments t_0 and $(t_0 + \Delta t)$, as depicted in Figure 3. A time dependency has been included now in all the parameters of equations (1) & (2). Based on equation (2), the time dependency of the projection measurements for a fan-beam scanner is expressed by

$$g_n(\sigma(t),\beta(t),t_o) = \iint f(x,y,t)\delta\{x\cos[\sigma(t)+\beta(t)] + y\sin[\sigma(t)+\beta(t)] - R\sin\sigma(t)\}dxdy, \tag{6}$$

where f(x,y,t), is a time varying tomography image. For CT applications, the amplitude difference between the two sets of measurements of equation (5) is defined by,

$$\Delta p_{n_o}(r,\theta,t_o+\Delta t) = p_{n_{s2}}(r(t),\theta(t),t_o+\Delta t) - p_{n_{s1}}(r(t),\theta(t),t_o), \text{ for } (n_o = 1,2,..,N-q). \tag{7}$$

For fan-beam scanners, the difference $\Delta g_{n_o}(\sigma(t),\beta(t),t_o+\Delta t)$, is defined by:

$$\Delta g_{n_o}(\sigma(t),\beta(t),t_o+\Delta t) = g_{n_{s2}}(\sigma(t),\beta(t),t_o+\Delta t) - g_{n_{s1}}(\sigma(t),\beta(t),t_o), \text{for } (n_o = 1,2,..,N-q). \tag{8}$$

As a result of equation (6), and recalling the spatial overlap concept of equation (5), which assumes that $\{\beta_{s1}(t_o+\Delta t)=\beta_{s2}(t_o)\}$, $\{\sigma_{s1}(t_o+\Delta t)=\sigma_{s2}(t_o)\}$, equation (8) takes the form:

$$\Delta g_n(\sigma(t),\beta(t),t_o+\Delta t) = \iint [f(x,y,t_o) - f(x,y,t_o+\Delta t)]\{\delta\{x\cos[\sigma_{s2}(t_o)+\beta_{s2}(t_o)] + y\sin[\sigma_{s2}(t_o)+\beta_{s2}(t_o)] - R\sin\sigma_{s2}(t_o)\}dxdy, \tag{9}$$

where $[f(x,y,t_o) - f(x,y,t_o+\Delta t)]$ indicates the tomography difference of the time varying image between the time moments t_0 and $(t_0 + \Delta t)$. If the measurements of the spatial overlap correlator depicted in Figure 3 and defined by equations (8) & (9) are provided at the input of an image reconstruction algorithm, then the image reconstruction process will reconstruct the time dependent image changes $[f(x,y,t_o) - f(x,y,t_o+\Delta t)]$ that will take place during the time period *T* of the CT data acquisition process.

If no motion is present the spatially overlapping measurements will be identical, and the measurements according to equation (9) will include zeroes, as expected. This suggests that the image reconstruction process of the spatially overlap correlator measurements of equation (9) will track only the moving components of the image. The stationary components will have zero contribution and they will not appear in the reconstructed image. This is confirmed by the results of Figure 5, which are discussed later. Figure 4, presents a graphical representation of the above two dimensional (2-D) space-time sampling process defined by equations (8) & (9) and Figure 3. The vertical axis shows the time moments associated with the angular positions of the source-array receiver, shown by the horizontal axis. The sets of line-segments along the diagonal, represent the measurements of a CT scanner.

Image reconstruction algorithms assumes stationarity in the image, or that these sets of measurements are along a horizontal line of Figure 4 (i.e. that they have been taken the same instant of time). However, as shown in Figure 4, during the T seconds period of a CT-

scanner's acquisition process, the image of interest may suffer deformation as is the case of organs motion (i.e. heart, lungs, etc.). In the same figure, the spatially overlapping measurements of equations (8) & (9), are depicted by the pair of lines that overlap in angular space but are taken at two successive time moments. This process is equivalent to a synthetic aperture processing scheme for SONAR applications [5,7]. An obvious organ motion correction process is to remove the temporal amplitude and phase differences, due to organ motion effects, between the spatially overlapping sets of measurements. Ideally, this correction process will correct the measurements with respect to the first measurement, which is equivalent in moving the diagonal measurements into the same instant in time and on the horizontal line, shown in Figure 4. This approach has been tested with synthetic data and it has been shown that it is not effective because the number M of projections in CT scanners is very large $O(10^3)$. As a result, the propagation of errors that are generated by the correction process build up significantly and begin to destroy useful information.

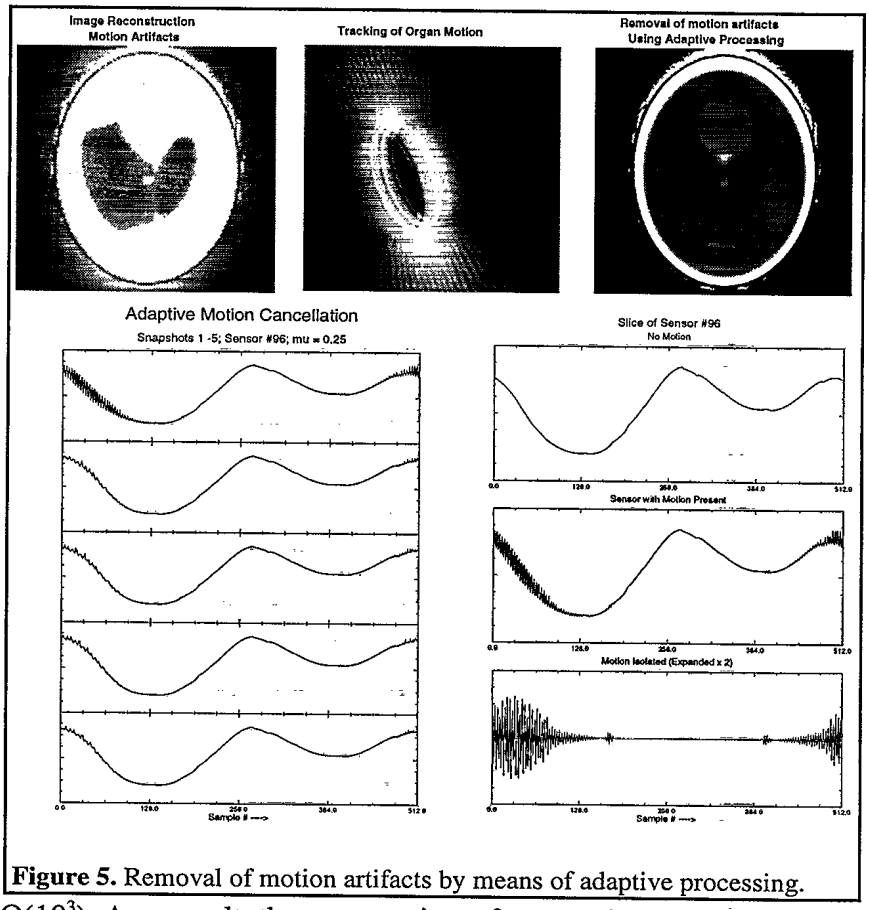

Figure 5. Removal of motion artifacts by means of adaptive processing.

III SYNTHETIC DATA

The simulations included the Shepp-Logan phantom as a test image. The software consisted of three standard components: (1) the projection data generation based on the phantom test image, (2) the image reconstruction algorithm, which was the filtered back-projection method including a Ram-Lak filter cascaded with the Parzen window, and (3) the image display. This is in addition to the signal processing components described in this paper. The geometry in the simulations and the rest of the parameters were equivalent with those of Elscint's CT Twin RTS medical tomography system. This is because the spatial overlap correlator has been tested with real data sets provided by Elscint for the above real time system.

The left hand side image of Figure 5, shows the reconstructed Shepp-Logan phantom that includes simulated motion for the left interior ellipse taking place during the data acquisition period of the CT scanner. The rest of the components of the phantom were assumed stationary. It is apparent by these results that the simulated motion induces blurring effects in the reconstructed image. The middle image of Figure 5 shows the output of the reconstruction process for the spatial overlap measurements that are expressed by equations (8) & (9). As expected, the reconstructed image includes the moving ellipse only. None of the stationary

components of the phantom appear in this reconstructed image. These results may be of important diagnostic value to track organ motion effects, and further may be used in processing schemes for motion artifact removal [4,5,8].

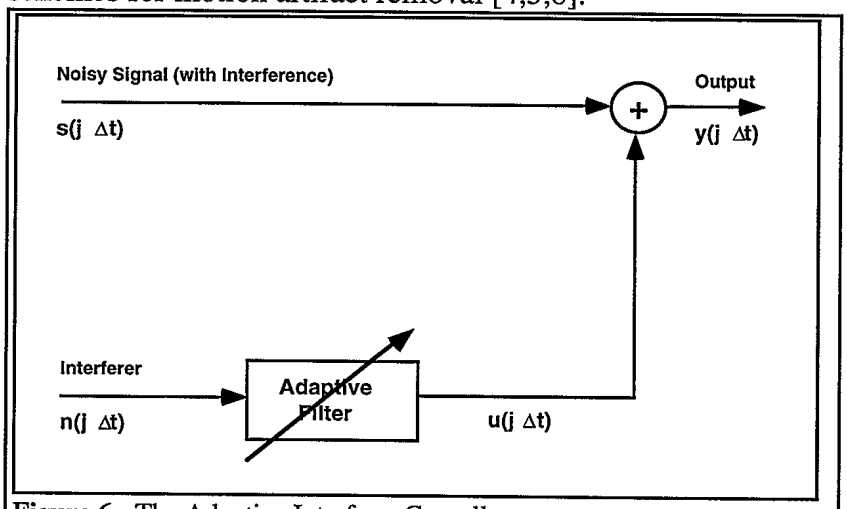

Figure 6. The Adaptive Interferer Canceller structure.

The lower right panel of Figure 5 shows the sensor time series of a typical sensor during the data acquisition process of a CT scanner's full 360° rotation. The top right curve is for a case with no motion present in the simulated phantom. The center right curve in the panel shows the same sensor time series with motion present for the left interior ellipse. It is apparent that the high frequency component, in this case, is associated with the simulated organ motion. The lower right curve shows the sensor time series provided by the overlap correlator. As expected, they include only the high frequency component associated with the organ motion.

Adaptive processing for Motion Artifact Removal The current focus of the investigation is to apply adaptive processing schemes [4,6,7] to remove the motion artifacts that have generated the fuzzy image shown at the left hand side of Figure 5. The structure of the Adaptive Interferer Canceller [6] is shown in Figure 6. This is a technique that is useful when any interferer that is present in a signal is accurately measured. The algorithms used in this investigation are the LMS and NLMS algorithms. They were chosen for their simplicity. The output of the Adaptive Interference Canceller (AIC) is given by $y(j\Delta t) = s(j\Delta t) - u(j\Delta t)$, (j = 1,2, ...,K), where K is the maximum number of samples to be processed. The output of the adaptive filter u(jΔt), for interferer input n(jΔt), and W adaptive weights (w_1, w_2, ... w_W) at time jΔt is given by equation (10).

$$u(j\Delta t) = \sum_{i=1}^{W} w_i^{j\Delta t} \times n\left(\left(j + i - \frac{W}{2}\right)\Delta t\right) \tag{10}$$

The adaptive weight update equations for the LMS and NLMS algorithms are given in (11) and (12) respectively.

$$w_i^{(j+1)\Delta t} = w_i^{j\Delta t} + \left(\mu \times n(j\Delta t) \times y(j\Delta t)\right), (i = 1,2,..., W), \tag{11}$$

where μ is the adaptive LMS step size parameter.

$$w_i^{(j+1)\Delta t} = w_i^{j\Delta t} + \left(\frac{\lambda}{|n|} \times n(j\Delta t) \times y(j\Delta t)\right), (i = 1,2,...W), \tag{12}$$

where λ is the NLMS step size parameter, α is a stability parameter, and |n| is the Euclidean norm of the vector

$$\left[n\left(\left(j+1-\frac{W}{2}\right)\Delta t\right), n\left(\left(j+2-\frac{W}{2}\right)\Delta t\right), ..., n\left(\left(j+\frac{W}{2}\right)\Delta t\right)\right].$$

The curves in Figure 7 show the operation of the AIC with the NLMS adaptive filter when there is accurate tracking of the interferer. The operation of this algorithm makes it an ideal tool for removing any motion artifacts present in the reconstructed image. Motion tracked at the sensor level by the overlap correlator (equivalent to the lower right curve of Figure 5) is introduced into the adaptive interferer canceller as the interference. The original sensor time series (equivalent to the center curve) are treated as the "noisy" signal at the input of the adaptive algorithm. The left lower panel of Figure 5 shows the sensor time series that result from adaptive processing. The left hand side waveforms demonstrate the results of the adaptive processing on the time series of the sensor when there is motion present.

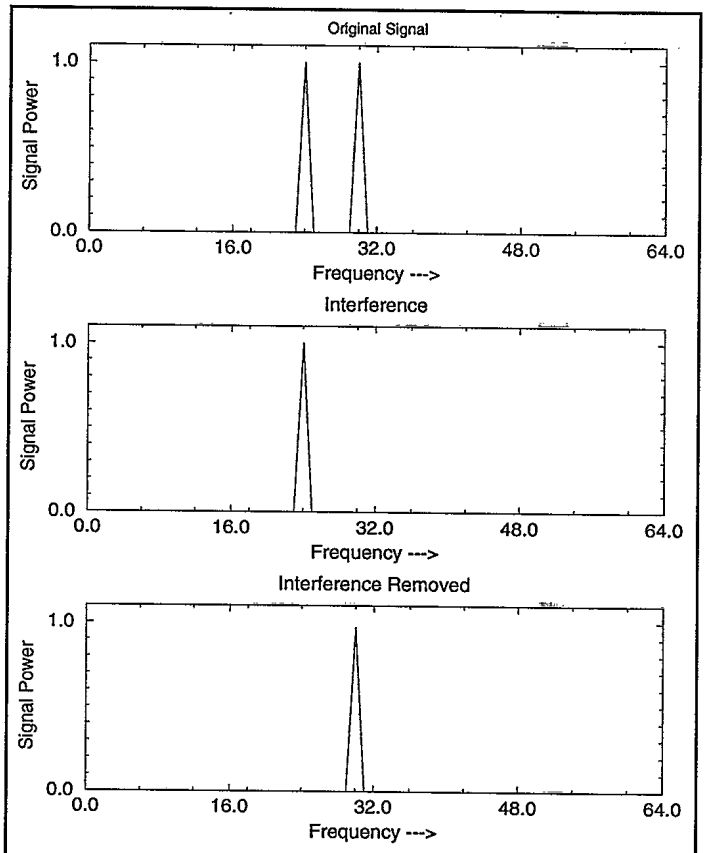

Figure 7. Output results of the Adaptive Interference Canceller's effects to remove noise interference signal.

To evaluate the effectiveness of the adaptive noise cancellation scheme, the spatial spectrum of the various types of time series, generated by the above processing, is shown in Figure 8. The upper part of Figure 8 shows the spatial spectrum of the "noisy" signal, corresponding to the center right curve in the lower panel of Figure 5, when there is motion of the left interior ellipse of the test phantom. The middle part of Figure 8 presents the spectrum of the times series output of the spatial overlap correlator, which corresponds to the lower right curve in Figure 5. The lower part of Figure 8 shows the spectrum of the time series output of the adaptive noise cancellation scheme, which corresponds to the left hand side lower curves of Figure 5. For comparison, the spectrum of time series, with no organ motion present, is shown in the same figure. It is apparent from the spectrum results of Figure 8 that the adaptive noise cancellation scheme suppresses the noisy components (associated with the organ motion) of the CT sensor data by as much as 40 dBs.

The iteration process of the adaptive processing shows the removal of the high frequency component of the organ motion from the sensor time series. Then image reconstruction on the new set of time series provides an image without motion artifacts as shown by the upper right hand side image of Figure 5. Although the above results may suggest that a low-pass spatial filter could have as been equally effective as the adaptive noise cancellation scheme to remove the high frequency components from the noisy signal, any attempt in that direction would demonstrate the following: A straight forward application of a low pass spatial filter on the time series of CT scanners could remove the high frequency components but it would destroy, as well, the small-size spatial structures in the associated tomography image. This approach was tested and it was found that the low pass filter is not effective to remove motion artifacts. Moreover it destroys the spatial resolution of the stationary components of a CT image. In this investigation, other issues, such as convergence of adaptive

schemes, will be addressed to provide a system solution. The final objective is to test the theoretical developments with real data sets.

IV SYSTEM IMPLEMENTATION: REAL DATA

Two Sources Concept for CT fan-beam scanners : An essential technical requirement by the spatial overlap correlator is the implementation of two CT X-ray sources separated with an angular spacing equal to the sensor spacing of the receiving array. However, because of the massive size of an X-ray source, the two source concept for a CT scanner is technically not feasible. At this point it is important to acknowledge the valuable contribution in this implementation effort by Elscint. In particular, the Elscint CT Twin RTS system includes the flying focal point functionality that is being used to double the spatial sampling frequency. Elscint [9] suggested that the second source can be generated by the deviation of the x-ray beam by a magnetic field, which is defined as a new active transmission of the source at an angle $\Delta\theta$ and time instant $\Delta t/2$ with respect to the previous source position. Typical values for $\Delta t/2$ are approximately 0.5ms, which provide spatial samples at _ the sensor spacing of the receiving array. This process is equivalent to doubling the spatial sampling frequency of a CT fan-beam scanner.

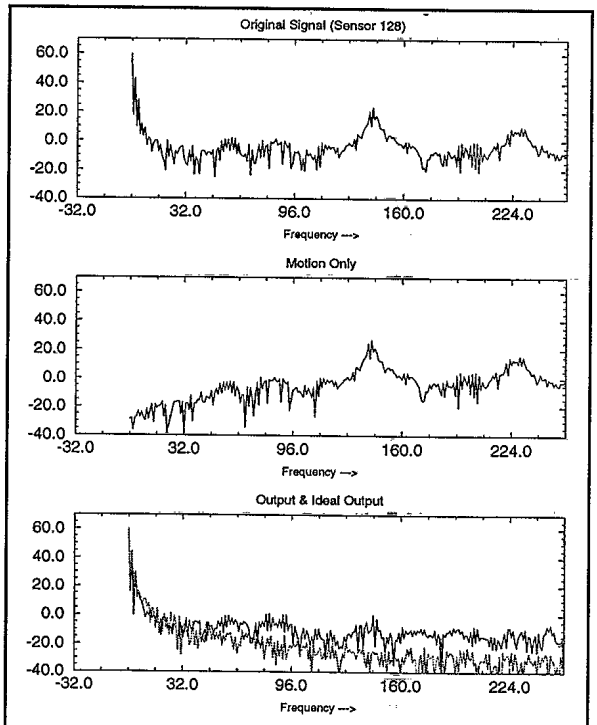

Figure 8. Spectrum of the various types of CT sensor time series shown in the lower panel of Figure 5.

The flying focal point functionality was modified in the Elscint CT Twin RTS system in such a way that will simulate the second source being activated about 0.5ms later than the previous X-ray transmission and at a location of _ sensor spacing with respect to the previous source activation. Although, this is not an ideal implementation effort, it may be viewed as the first step towards a system oriented solution and implementation of the spatial overlap correlator concept. In Elscint's implementation effort of the two source concept, the sensor time series associated with each one of the flying focal point X-ray source transmissions had to be distinguished in such a way as defined by equation (8). Then, the time series without any kind of pre-processing or image reconstruction were provided at the input of the proposed processing scheme that is shown in Figure 10.

Implementation of Spatial Overlap Correlator in CT systems without Flying Focal Point: The requirement of the flying focal point functionality regarding the implementation of the spatial overlap correlator in a CT system, is a serious restriction for a wide range of CT system oriented applications. This is because, the flying focal point functionality exists only in Siemens' and Elscint's latest CT systems. In what follows, an attempt is being made to replace the two source requirement associated with the spatial overlap correlator.

Let us start with the physical interpretation of the concept of Figure 3. The two source concept is equivalent to the procedure of taking two successive pictures of the same scenery or view. If the view includes movement of objects during the time interval separating the acquisition process of the two pictures, then the two pictures will not be identical. In this case, application of the spatial overlap correlator concept requires tracking any amplitude (or intensity) difference, that is due to movement of objects, between the two pictures,. This process is illustrated in Figure 9 and includes the following steps.

First, the time series segment (sinogram) associated with the full rotation of the CT scanner and the reconstruction of a complete image, are defined as: $Z_n(j\Delta t)$, (n=1,2,..,N & j=1,2,...,M), where N is the number of sensors of the receiving array of the CT system and M are the number of projections during one full rotation of the scanner. The above time series, when are inserted at the input of the filter back-projection algorithm (F.B-P.A) they will provide a reconstructed image f(x,y) associated with the CT measurements, as discussed above.

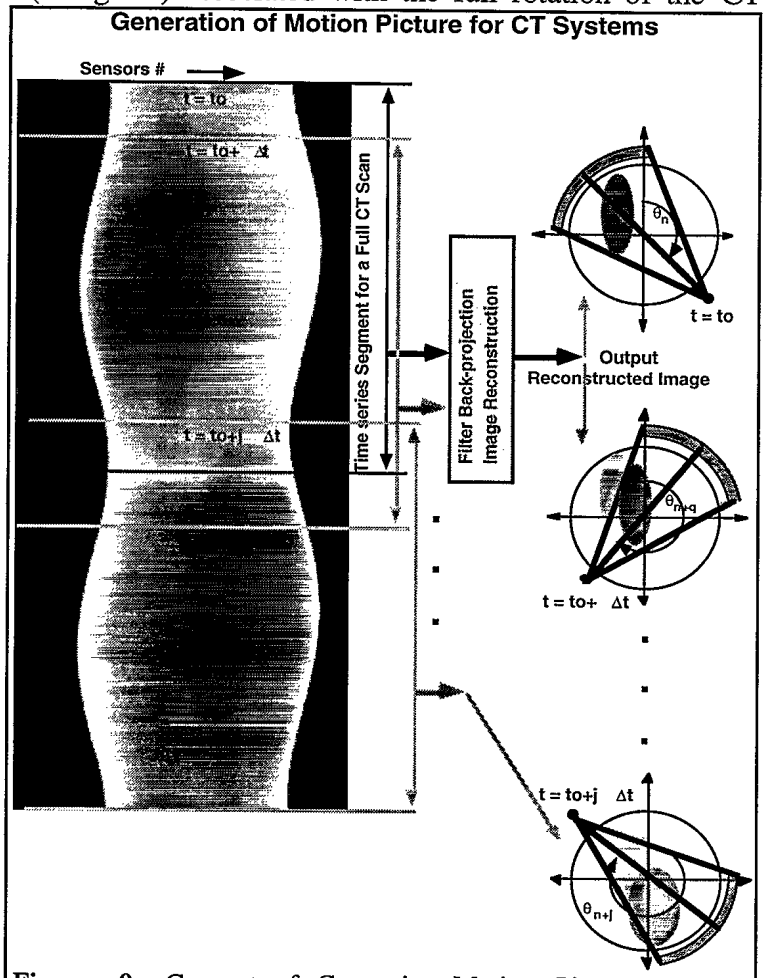

Figure 9. Concept of Generating Motion Pictures for CT systems capable to track organ motion.

Second, the next set of time series, Δt seconds later and defined by, $Z_n(j\Delta t)$, (n=1,2,..,N & j=2,...,M+1), when inserted in the (F.B-P.A) they will provide a reconstructed image $f(x,y,\Delta t)$ with differences associated with the Δt seconds time interval, with respect to the previous one. A difference between the above two reconstructed images would require rotation and alignment of the second image to coincide with the same view as the first one. However, since the (F.B-P.A) is a linear operator, the difference between the above two images $\{f(x,y,\Delta t) - f(x,y)\}$ corresponds to the amplitude difference of the associated time series defined above. Thus, this kind of time series difference, when the appropriate image rotation is taken into account, is defined by: $\Delta Z_n(j\Delta t)= \{Z_n[(M+j)\Delta t] - Z_n(j\Delta t)\}$, (n=1,2,..,N & j=1,2,....). If the time series $\Delta Z_n(j\Delta t)$, was inserted at the input of the (F.B-P.A), an image will be reconstructed tracking organ movement taking place during the period $M\Delta t$ seconds of the CT data acquisition.

Although this process may seem identical with the spatial overlap correlation process of Figure 3, there are two fundamental differences between them that may have implications on the implementation of the adaptive noise cancellation scheme. The first difference is that the second

methodology tracks organ movement differences that are separated by an initial period of $T=M\,\Delta t$ seconds. The second difference is related to the initial phase of the organ movement, which will be out of phase with respect to the starting point of the CT data acquisition process. As a result, the adaptive noise cancellation scheme may not be effective, because the interference noise (i.e. $\Delta Z_n(j\Delta t)$, $(n=1,2,..,N \;\&\; j=1,2,....)$) will be out of phase (or slightly irrelevant) with respect to the noisy signal: $Z_n(j\Delta t)$, $(n=1,2,..,N \;\&\; j=2,...,M+1)$. More efforts are being invested in this area to examine a generic implementation concept of the spatial overlap correlator and the adaptive noise cancellation scheme in CT applications.

Real data: The real data results of the system implementation effort were quite promising and included the tracking of an irregular-oscillatory motion of a real test phantom. The real data results included the continuous tracking of the phantom motion (organ motion) during the time interval of 30 seconds. This is equivalent in producing a motion picture of the organ motion as is the case in ultrasound medical imaging systems. Thus, the 30 seconds CT results included a set of 300 images separated by 1/10 seconds time interval. Continuous viewing of the 300 images produced a motion picture that indicated clearly the irregular oscillatory motion of the phantom. Figure 9 depicts schematically the concept of generating a motion picture for CT systems capable to track organ motion as proposed in this paper. In this case, the time interval $\Delta\tau$ was equal to 0.1 seconds.

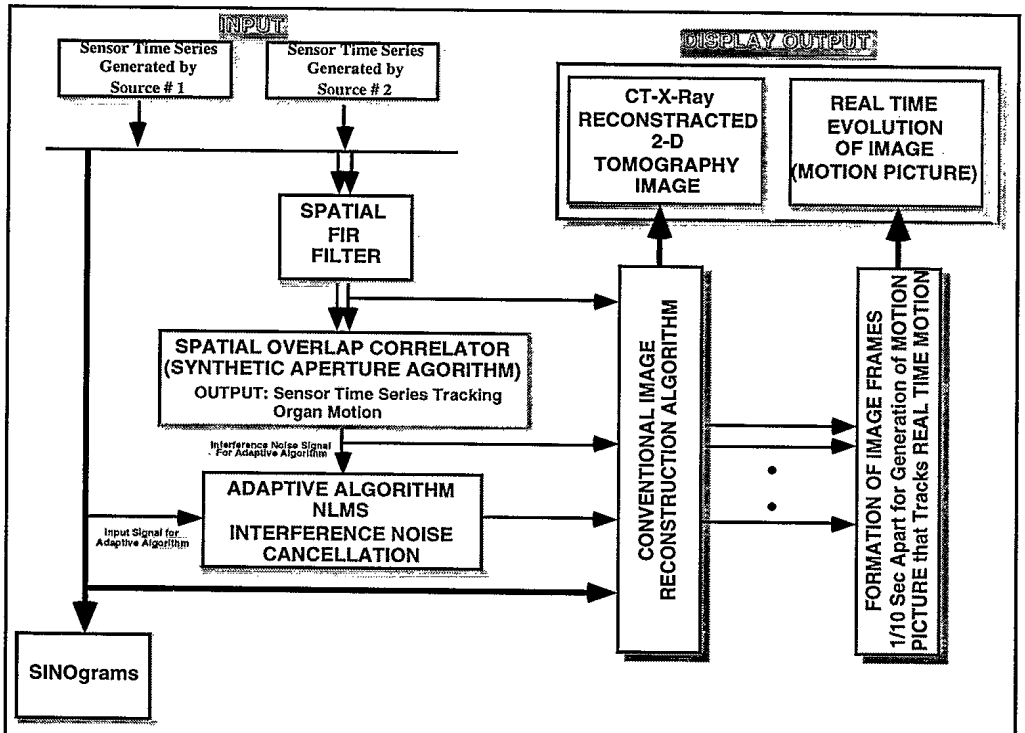

Figure 10. Signal processing flow for a X-ray CT system including the spatial overlap correlator and the adaptive interference noise cancellation scheme to correct for motion artifacts.

Finally, Figure 10 presents the processing flow as it is defined for an X-ray CT system including the spatial overlap correlator, the adaptive interference cancellation scheme, the filter back-projection image reconstruction algorithm and the dual display including the conventional X-ray CT images and the motion picture to track and view the organ motion as a function of time. The unshaded blocks represent the current signal processing flow of CT systems. The shaded blocks indicate the proposed signal processing schemes required by a CT system to achieve the motion picture functionality in terms of tracking organ motion and monitoring & distinguishing stationary and moving components of tomography images in CT applications.

V CONCLUSION

The paper discusses a novel approach to tracking and removing organ motion artifacts in CT systems. The method first uses the overlap correlator processing scheme to sample information associated with the organ motion present during the CT data acquisition process. The classic adaptive interference noise cancellation method is then used to remove these motion effects, which are treated as noise interference at the input of the adaptive processor. Tests with real and synthetic data sets demonstrate the validity of the proposed signal processing methodology, and also proves that it is practically realizable.

ACKNOWLEDGMENT

The authors wish to express their appreciation to Dr. Dov Maor, Chief Scientist of Elscint CT (Haifa, Israel) and the technical experts of Elscint for the technical discussions and exchanges on the subject matter, as well as their effort to modify the operation of their latest CT Twin RTS system and allow the implementation of the spatially overlap correlator to generate the real data sets for the testing of the proposed concept.

REFERENCES

[1] Srinivas, C., Costa, M. H. M., "Motion-Compensated CT Image Reconstruction", Proceedings of the IEEE Ultrasonics Symposium, **1**, pp. 849-853, 1994.

[2] Chiu, Y. H., Yau, S. F., "Tomographic Reconstruction Of Time Varying Object From Linear Time-Sequential Sampled Projections", *Proceedings of the IEEE*, 0-7803-1775-0/94, pp. 309 - 312, 1994.

[3] Hedley, M., Yan, H., Rosenfeld, D., "Motion Artifacts Correction in MRI Using Generalized Projections", *IEEE Transactions on Medical Imaging*, **10**(1), pp. 40-46, 1991.

[4] Dhanantwari, A., & Stergiopoulos, S., *Proceedings ICA/ASA'98, J. Acoust. Soc. Am.* **103**(2), Pt.2, 28, 1998.

[5] Stergiopoulos, S., *J. Acoust. Soc. of Am.*, **90**(6), 3161-3172, 1991

[6] Widrow, B., Stearns S. D., Adaptive Signal Processing, Prentice - Hall, 1985

[7] Stergiopoulos, S., *Proceedings of the IEEE*, **86**(2), 358-396, February (1998).

[8] Stergiopoulos S., (Technical Project Manager), "EC-Esprit, EP 26764 New Roentgen project", Oct., 1997.

[9] Maor, Dov, (Chief Scientist, Elscint CT, Haifa, Israel), "Results of EC-Esprit, EP 26764 New Roentgen project", Feb., 1998.

[10] Kak, A. C., Digital Image Processing Techniques, Academic Press, New York, 1984.

[11] F.J. Harris, *Proceedings of the IEEE*, **66**, 51-83, 1978.

#510036